The Spectral Element method for elastic wave equations: application to 2D and 3D seismic problems

Dimitri Komatitsch, Jeroen Tromp, EPS, Harvard University and Jean-Pierre Vilotte, IPGP*

Summary

We present a spectral element method to simulate elastic wave propagation in realistic geological structures involving interfaces and steep topography for 2D and 3D geometries. The spectral element method is a high-order variational approximation of the elastic wave equation. The mass matrix is diagonal by construction, which drastically reduces the computational cost. The time discretization is based on a Newmark scheme written in a predictor/multi-corrector format. A spatial sampling of approximately 4 or 5 points per wavelength is found to be very accurate. This fact is demonstrated by comparing the computed solution to the analytical solution of the classical 2D problem of an explosive source in a half-space. The flexibility of the method is illustrated by studying a realistic two-dimensional model with steep topography (mountain ranges). The method is also shown to provide an efficient tool for studying the diffraction by 3D topography and the associated effects on ground motion.

Introduction

The use of elastic wave equations to model the seismic response of heterogeneous geophysical media with topography and complex interfaces is a subject that has been intensively investigated. The challenge is to develop high performance methods capable of solving the elastic wave equations accurately, and that are capable of dealing with large and complicated domains as encountered in realistic 3D applications.

Finite difference methods (Virieux, 1986) have been widely implemented with a varying degree of sophistication. Unfortunately, conventional schemes suffer from grid dispersion near large gradients of the wavefield or when too coarse computational grids are used. Although more suited to heterogeneous media with complicated geometries, finite element methods have attracted less interest in geophysics due to the fact that low-order finite element methods exhibit poor dispersion properties (Marfurt, 1984), while higher order classical finite elements lead to some problems such as the occurrence of spurious waves. Boundary integral representations of the problem (Bouchon et al., 1996) are often very accurate but unfortunately limited to linear and homogeneous problems. Moreover, the resulting linear systems of equations are very large, non-symmetric and dense, which makes their application to 3D problems difficult. Pseudospectral methods have also been proposed for elastodynamics (Carcione and Wang, 1993), but suffer from important limitations: non-uniform spacing of the collocation points puts stringent constrains on the time-step that cannot be easily removed, and as in any global method, only smooth topography can be handled.

Therefore, here we use a spectral element method (Patera, 1984; Priolo et al., 1994; Komatitsch and Vilotte, 1998) to solve the 2D and 3D elastic wave propagation in complex geometries. The method, which derives from a weak variational formulation, allows a flexible treatment of boundaries and interfaces, and deals with free-surface boundary conditions naturally. It combines the geometrical flexibility of a low-order method with the exponential convergence rate associated with spectral techniques, and suffers from minimal numerical dispersion and diffusion.

The Spectral Element Method

We consider the variational formulation of the elastodynamic equation. The most commonly used formulation is based on the principle of virtual work and can be written using the displacement vector $\mathbf{u}$ and the test function $\mathbf{w}$ as (Hughes, 1987):

$$(\mathbf{w}, \rho\ddot{\mathbf{u}}) + a(\mathbf{w}, \mathbf{u}) \;=\; (\mathbf{w}, \mathbf{f}) \qquad (1)$$

where $a(\cdot,\cdot)$ denotes the bilinear form that expresses the virtual work of the internal stresses, defined as :

$$a(\mathbf{w}, \mathbf{u}) \;=\; \int_{\mathbf{\Omega}} \boldsymbol{\sigma} : \nabla \mathbf{w} \, dV = \int_{\mathbf{\Omega}} \nabla \mathbf{w} : \mathbf{c} : \nabla \mathbf{u} \, dV \qquad (2)$$

where $\boldsymbol{\sigma}$:$\nabla \mathbf{w} = \sigma_{ij} \partial w_i / \partial x_j$ and $\mathbf{c}$ is the stiffness tensor. Like in a standard finite element method, the original domain is discretized into n_{el} non-overlapping quadrilateral elements: $\bar{\mathbf{\Omega}} = \bigcup_{e=1}^{n_{el}} \bar{\mathbf{\Omega}}_e$. Each element $\bar{\mathbf{\Omega}}_e$ is mapped onto a reference volume $\square$ that is defined, in a local $\boldsymbol{\xi}$-system of coordinates, as a square or a cube Λ^{n_d} with $\Lambda = [-1, 1]$. Each element integral, defined over the domain $\bar{\mathbf{\Omega}}_e$ in the physical space, is pulled back, using a local mapping $\mathcal{F}_e$, on the parent domain $\square$ and numerically integrated using the numerical quadrature defined as the tensor-product of the 1D Gauss-Lobatto-Legendre formulas. The $(N+1)^{n_d}$ basis points for the polynomial basis are taken to be the same as the quadrature points on each element $\bar{\mathbf{\Omega}}_e$, and define a local collocation grid $\Xi_N^e = \{\xi_i, \eta_j, \zeta_k\}$ that is the n_d-tensor product of the $N+1$ Gauss-Lobatto-Legendre integration points.

The piecewise-polynomial approximation $\mathbf{w}_N^h$ of $\mathbf{w}$ is defined using the Lagrange interpolation operator $\mathcal{I}_N$ on the Gauss-Lobatto grid Ξ_N^e : $\mathcal{I}_N(\mathbf{w}|_{\bar{\mathbf{\Omega}}_e})$ is the unique polynomial of $\mathbb{P}_N(\square)$ which coincides with $\mathbf{w}|_{\bar{\mathbf{\Omega}}_e}$ at the $(N+1)^{n_d}$ points of Ξ_N. If $l_i^N(\xi)$ denotes the characteristic Lagrange polynomial of degree N associated with the

Gauss-Lobatto point i of the 1D quadrature formula, the approximation of $\mathbf{w}|_{\bar{\Omega}_e}$ is defined as :

$$\mathbf{w}_N^h|_{\bar{\Omega}_e}(\mathbf{x}) = \sum_{i,j,k=0}^{N} l_i^N(\xi) l_j^N(\eta) l_k^N(\zeta)\, w_{ijk}^e \qquad (3)$$

with $\mathbf{x} = \mathcal{F}_e(\xi_i, \eta_j, \zeta_k)$ and $w_{ijk}^e = \mathbf{w}_N^h|_{\bar{\Omega}_e} \circ \mathcal{F}_e(\xi_i, \eta_j, \zeta_k)$. This procedure leads, like in the finite element method, to a coupled system of ordinary differential equations :

$$\mathbf{M}\,\ddot{\mathbf{u}}_t = \mathbf{F}_t^{ext} - \mathbf{F}_t^{int}(\mathbf{u}_t). \qquad (4)$$

We use n_{node} to denote the total number of nodes of the global integration grid Ξ_N defined as the assembly of the element domain integration grids $\Xi_N = \bigcup_e \Xi_N^e$; $\mathbf{u}_t$ denotes the global displacement vector at a given time t; $\mathbf{F}^{int}$ is the internal nodal force vector, and $\mathbf{F}^{ext}$ the external source term. The mass matrix $\mathbf{M}$ is diagonal by construction. This system is then discretized in time using a classical second-order Newmark scheme (Hughes, 1987) written in predictor-multicorrector format.

The spectral element method combines the geometric flexibility of the finite element method with the fast convergence associated with spectral techniques. The discrete solution suffers from minimal numerical dispersion and diffusion, a fact of primary importance in the solution of realistic geophysical problems. In practice, a spatial sampling of approximately 4 or 5 points per minimum wavelength is found very accurate when working with a polynomial degree $N = 8$. Typically , for 2D simulations with a 100,000 points curvilinear grid, the memory occupation is of the order of 30 Megabytes and the CPU time, for a simulation over 2000 time steps, is of the order of 15 minutes on an UltraSparc-1. For large 3D simulations, using a 5,000,000 points curvilinear grid, the memory occupation is of the order of 1 Gigabyte and the CPU time is of the order of 1 or 2 hours on a parallel computer.

Garvin's problem

Garvin's problem (Garvin, 1956) is a classical test to check the accuracy of a wave propagation code. An homogeneous elastic half-space is considered, with a compressive source (explosion) placed exactly at the surface. There exists an analytical solution to this problem. The main event is the propagation of a strong Rayleigh wave along the surface. The Rayleigh pulse is non dispersive, as the medium is homogeneous and the surface is flat. Its amplitude remains constant in the case of plane strain. The corresponding snapshots are presented on Figure 1, and the seismograms on Figure 2, the receivers being located at the free surface. One can observe the direct P wave, the strong Rayleigh wave with its typical elliptical polarization, and the head wave. Comparison with the analytical solution at receiver 100 at the end of the line is displayed on Figure 3. Very good agreement is found, the maximum relative error being less than 1 %.

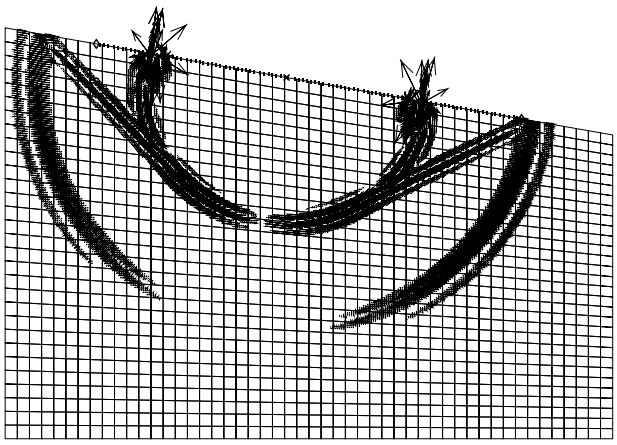

Fig. 1: Snapshots for tilted Garvin's problem with an explosive source placed at the free surface. The strong Rayleigh wave with its typical elliptical polarization can be clearly observed, as well as the head wave.

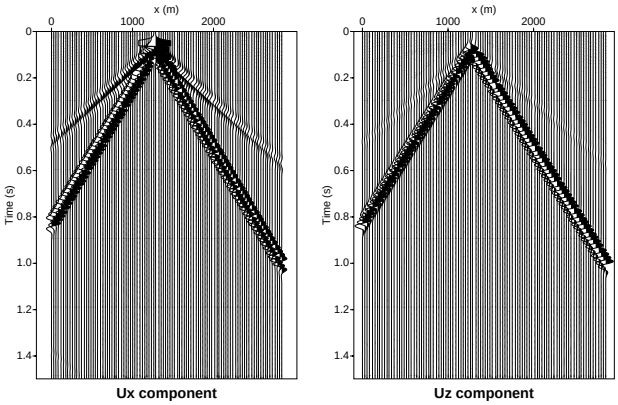

Fig. 2: Seismograms for tilted Garvin's problem with an explosive source placed at the free surface. The main event is a strong non dispersive Rayleigh wave. No significant numerical noise can be observed.

Realistic model in South America

It is also interesting to study a more realistic example. We consider a geological structure in the Andes (courtesy Elf Aquitaine). The width of the model is 5500 m, and the "average" height of the topography is roughly 1300 m. The mesh is shown on Figure 4. It is composed of 60×12 elements, using a polynomial degree of 8. The total number of points is 46657. The source is an explosion inside the model at $(x, z) = (1000, 670)$ m. Its time dependence is a Ricker wavelet having a central frequency of 12 Hz. The line of receivers is placed at the free surface between $x = 900$ and $x = 5000$ m.

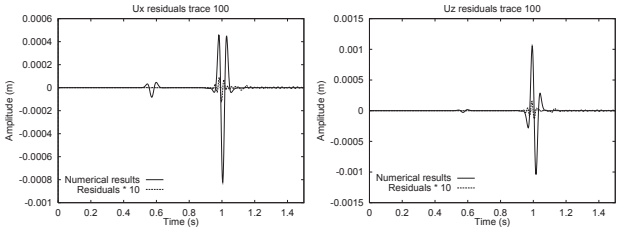

Fig. 3: Trace recorded at receiver 100 for tilted Garvin's problem with an explosive source placed at the free surface. The numerical solution is plotted together with the residuals with respect to the analytical solution drawn at the same scale after multiplication by a factor of 10. The agreement is very good, the maximum error being of the order of 1 %.

In order to estimate the effect of the rough topography on the wavefronts, we first simulate the propagation using a homogeneous velocity and density model. The P velocity is 3200 m.s^{-1}, the S velocity is 1847.5 m.s^{-1} and the density is 2200 kg.m^{-3}. The time step is $\Delta t = 0.30$ ms, the total number of time steps is 5000. Snapshots of the displacement vector are presented on Figure 4. Even for this homogeneous model, the effect of the topography is very important, generating some strong diffracted phases that are superimposed to the direct waves.

We now use the "real" velocity model estimated for the structure, and display a snapshot of the divergence and curl of the displacement on Figure 4, and the seismograms on Figure 5. The complex shape of the signal can be observed, including numerous reflections and conversions at curved interfaces inside the model, in addition to the diffraction from the topography that has been observed in the homogeneous case, and that still appears clearly on the seismograms.

Amplification by a three-dimensional hill

To illustrate the capabilities of the spectral element method for 3D problems, we now study the diffraction of elastic waves by a hill. This study is motivated by some recent results obtained using Boundary Integral methods (Bouchon et al., 1996) and allows us to show that the spectral element method is an efficient tool to investige the diffraction of elastic waves by 3D structures.

The hill has a Gaussian shape, the size of the model is 2080 × 2080 × 1050 m, and the mesh is composed of 26 × 26 × 14 elements, with a polynomial order of $N = 8$, corresponding to a total number of 4935953 points (Figure 6). A homogeneous medium is considered, with a P wave velocity of 3200 m.s^{-1}, a S wave velocity of 1847.5 m.s^{-1}, and a density of 2200 kg.m^{-3}. The structure is excited by a vertically incident plane S wave polarized along the minor axis of the topography. The source is a Ricker wavelet in time, with a fundamental frequency of $f_0 = 10.2$ Hz. The simulated time interval is 0.8 s, with a time step of $\Delta t = 0.5$ ms. Periodic boundary conditions are implemented on the lateral edges of the grid to simulate a plane wave in a semi-infinite domain.

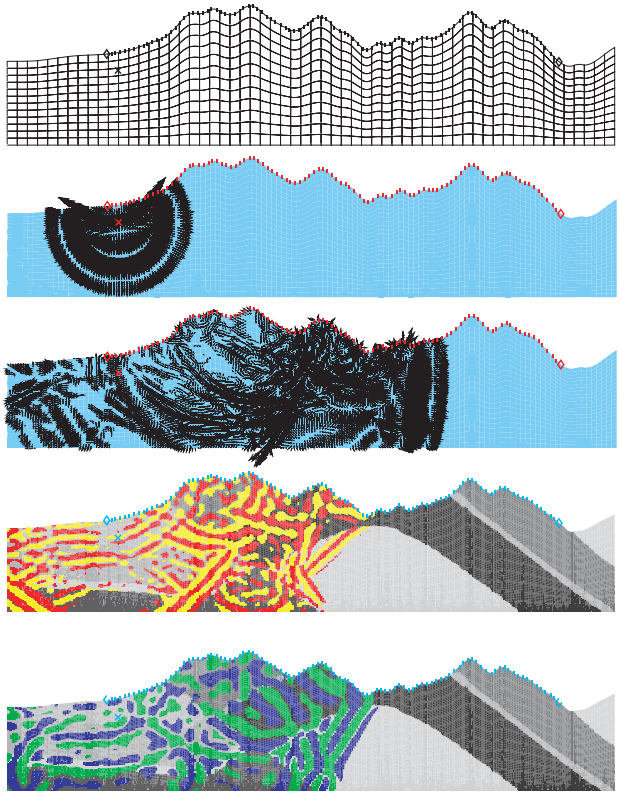

Fig. 4: Snapshots showing wave propagation for a section across the Andes (courtesy Elf-Aquitaine). The displacement vector and the real topography (with no vertical exaggeration) are displayed, illustrating the grid (top), the homogeneous results (middle) and the heterogeneous results (bottom). The effect of the topography is very important, with diffracted phases generated by the different peaks, and numerous reflections and conversions at the interfaces inside the model.

Figure 7 shows the surface ground motion recorded along the minor and major axes of the topography. The main features are strong amplification near the summit, and very clear diffracted waves, away from the topography, composed of a surface P wave and a Rayleigh wave. In the vicinity of the hill, the amplitude of the Rayleigh wave is of the same order as that of the P wave but, as it propagates, the P wave amplitude decreases faster, and the Rayleigh wave becomes the dominant feature. A strong directivity effect induced by the topography is observed, since the diffracted waves clearly propagate preferentially along the minor axis.

Conclusions

An efficient spectral element method for calculating the propagation of seismic waves through 2D and 3D geological structures has been presented. The method is based on a high-order variational formulation of the elastodynamics equations that allows a natural treatment of an irregular free surface. A classical 2D problem having an analytical solution has been studied to assess the

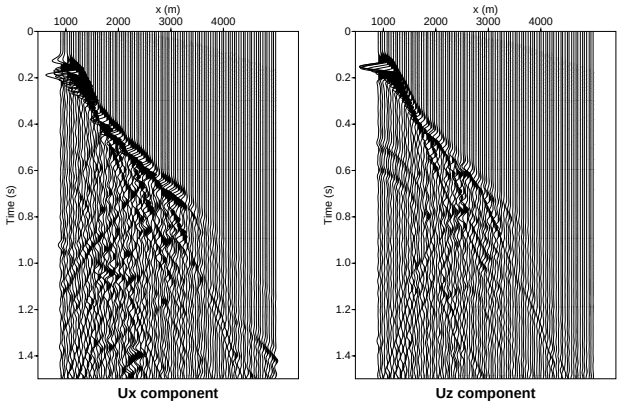

Fig. 5: Seismograms obtained for the realistic model in the Andes using the "real" velocity model. Diffraction from the topography is particularly clearly .

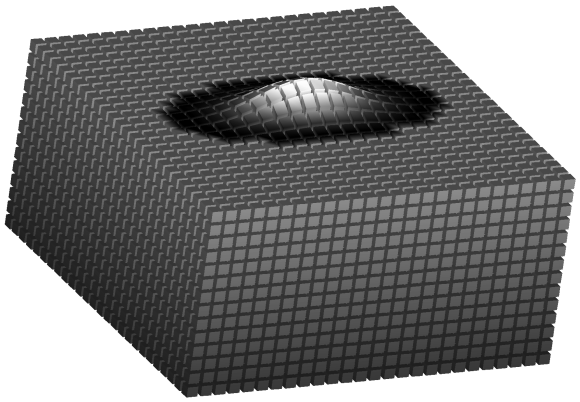

Fig. 6: Three dimensional model : a Gaussian-shaped hill is superimposed on an homogeneous elastic half-space. The total number of collocation points is 4935953.

accuracy of the method. The discrete solution presents minimal numerical dispersion. High accuracy is obtained using only 4 or 5 points per minimal wavelength. The capability of the method to handle complex free-surface geometries and deformed internal interfaces have been illustrated by solving a realistic 2D problem involving a mountain range. Finally, the spectral method has been shown to be an efficient tool to study the diffraction of elastic waves by 3D topography and its effect on ground motion.

Acknowledgements

The authors would like to thank F. J. Sánchez-Sesma, R. Madariaga, E. Chaljub, E. Priolo and G. Seriani for numerous fruitful discussions. G. Moguilny provided an invaluable help for the graphics.

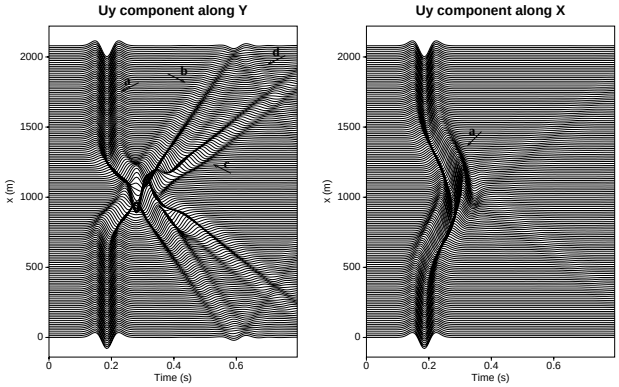

Fig. 7: Seismograms of the horizontal component of the displacement vector at receivers placed on the free surface, along the minor (left) and major (right) axes of the 3D topography. In addition to the direct wave (a), a strong directivity effect is observed on the diffracted P (b) and Rayleigh (c) waves that are recorded mainly along the minor axis. Some artefacts due to the periodic boundary conditions (d) are also observed.

References

Bouchon, M., Schultz, C. A., and Toksoz, M. N., 1996, Effect of three-dimensional topography on seismic motion: J. Geophys. Res., **101**, 5835–5846.

Carcione, J. M., and Wang, P. J., 1993, A Chebyshev collocation method for the wave equation in generalized coordinates: Comp. Fluid Dyn. J., **2**, 269–290.

Garvin, W. W., 1956, Exact transient solution of the buried line source problem: Proc. R. Soc. London Ser. A, **234**, 528–541.

Hughes, T. J. R., 1987, The finite element method, linear static and dynamic finite element analysis: Prentice-Hall International, Englewood Cliffs, NJ.

Komatitsch, D., and Vilotte, J. P., 1998, The spectral element method: an efficient tool to simulate the seismic response of 2D and 3D geological structures: Bull. Seis. Soc. Am., in press.

Marfurt, K. J., 1984, Accuracy of finite-difference and finite-element modeling of the scalar waveequation: Geophysics, **49**, 533–549.

Patera, A. T., 1984, A spectral element method for fluid dynamics: laminar flow in a channel expansion: J. Comput. Phys., **54**, 468–488.

Priolo, E., Carcione, J. M., and Seriani, G., 1994, Numerical simulation of interface waves by high-order spectral modeling techniques: J. Acoust. Soc. Am., **95**, no. 2, 681–693.

Virieux, J., 1986, *P-SV* wavepropagation in heterogeneous media: velocity-stress finite-difference method: Geophysics, **51**, 889–901.